Contribution of organic anion transporting polypeptide OATP2B1 to amiodarone accumulation in lung epithelial cells

Satoru Seki, Masaki Kobayashi, Shirou Itagaki, Takeshi Hirano, Ken Iseki *

Department of Clinical Pharmaceutics and Therapeutics, Graduate School of Pharmaceutical Sciences, Hokkaido University, Kita-12jo, Nishi-6-chome, Kita-ku, Sapporo 060-0812, Japan

ARTICLE INFO

ABSTRACT

The accumulation mechanisms of amiodarone (AMD) involving transporters in lung alveolar epithelial type II cells were studied. The uptake of AMD was examined using human alveolar epithelial-derived cell line A549 as a model. AMD was transported by the carrier-mediated system, and the apparent K_m and V_{max} values were 66.8 ± 30.3 μM and 49.7 ± 9.7 nmol/mg protein/5 min, respectively. The uptake of AMD by A549 cells was Na^+-independent and was inhibited by substrates of human organic anion transporting polypeptide (OATP). The inhibition profiles were similar to the inhibitory effects of several compounds on OATP2B1-mediated E-3-S transport, and RT-PCR analysis showed mRNA expression of OATP2B1 and 1B3 in A549 cells. SiRNAs targeted to the *OATP2B1* gene decreased the OATP2B1 mRNA expression level in A549 cells up to about 50% and reduced the uptake of AMD up to about 40%. These results indicate that AMD uptake mediated by carriers, including OATP2B1, might lead to accumulation of AMD in the lung and AMD-induced pulmonary toxicity (AIPT).

© 2009 Elsevier B.V. All rights reserved.

1. Introduction

Amiodarone (AMD) is a benzofurane derivative with class III antiarrhythmic activity that is effective in controlling intractable cardiac arrhythmias [1,2]. Clinical evidence suggests that this drug has a role in reducing the relative risk for arrhythmic or sudden death and overall mortality in survivors of myocardial infarction and in heart failure patients [3–7]. Among the various antiarrhythmic agents, AMD has electrophysiological effects that most closely approximate those of an ideal antiarrhythmic agent [8]. Although AMD is used widely [9], there is a risk of development of life-threatening AMD-induced pulmonary toxicity (AIPT) [10]. AIPT has been clinically diagnosed in 5 to 10% of patients receiving high doses of AMD and in 1.6% of patients receiving AMD at a dose of 400 mg/day or less [11]. Because of its high potential for mortality, AIPT is the adverse event of greatest concern for patients receiving AMD therapy.

Several mechanisms responsible for AIPT, including alteration in inflammatory mediator release [12], cell membrane perturbation [13] and phospholipids promotion [14], have been proposed. It has also been reported that AMD appears to activate a specific intracellular death-related pathway, including passively the bax-dependent caspase-3 activation pathway, and thus induce apoptosis in human lung epithelial cells [15]. Bolt et al. reported that AMD-induced perturbations of mitochondrial function may initiate AIPT [16].

Thus, the mechanisms of AIPT and AMD-induced cytotoxicity have been extensively studied. On the other hand, AMD has a strong tendency to accumulate in the lung among lean tissues [17–20]. This characteristic tissue distribution of AMD is also considered as a factor responsible for the initiation of AIPT, and an uptake mechanism(s) of AMD is presumed to exist in lung tissue. Although it was believed that AMD absorption is mediated by a passive diffusion process [21], the second highest rate of AMD accumulation in the lung after that in adipose tissue cannot be explained. AMD has been reported to be an inhibitor of P-gp [22,23] and rat organic anion transporting polypeptide 2 (Oatp2) [23,24], but the transport mechanisms of AMD itself have not been elucidated.

Thus, we focused on the uptake mechanisms of AMD involving transporters in lung alveolar epithelial cells. In this study, we characterized the transport mechanisms of AMD using the human alveolar epithelial-derived cell line A549, which is used widely in AMD toxicity experiments. We also showed that human organic anion transporting polypeptide 2B1 (OATP2B1) contributes to AMD uptake in A549 cells.

2. Materials and methods

2.1. Chemicals

AMD was kindly supplied by Taisho Pharmaceutical (Tokyo, Japan). [³H] Estrone-3-sulfate (E-3-S) was purchased from Perkin Elmer (Waltham, MA). All other reagents were of the highest grade available and used without further purification. AMD was dissolved in methanol (1% w/v final concentration) due to its hydrophobic properties and poor solubility in water.

* Corresponding author. Tel./fax: +81 11 706 3770.
E-mail address: ken-i@pharm.hokudai.ac.jp (K. Iseki).

Table 1
Primer sequences for RT-PCR and real-time PCR.

Gene	Primer sequence	Product size (bp)	Reference
OATP1A2	Forward 5′-AAGACCAACGCAGGATCCAT-3′ Reverse 5′-GAGTTTCACCCATTCCACGTACA-3′	101	[26]
OATP2B1	Forward 5′-GAGTTTCACCCATTCCACGTACA-3′ Reverse 5′-GCCACAGGACTCCATGCCT-3′	198	[27]
OATP1B1	Forward 5′-TGTCATTGTCCTTTTACCTATTAT-3′ Reverse 5′-TGTAAGTTATTCCATTGTTTCCAC-3′	195	[28]
OATP3A1	Forward 5′-CAGGCCATGCTCTCCGAAA-3′ Reverse 5′-CTGCTGCTCCAGGTACTTCC-3′	237	Present study
OATP4A1	Forward 5′-CTGCCAGCCAGAACACTACA-3′ Reverse 5′-AGAAGGAGGGGCTTTCTCTG-3′	216	Present study
OATP1B3	Forward 5′-GTCCAGTCATTGGCTTTGCA-3′ Reverse 5′-CAACCCAACGAGAGTCCTTAGG-3′	111	[26]

2.2. Cell culture

A549 cells obtained from American Type Culture Collection (Rockville, MD) were maintained in plastic culture flasks (Falcon, Becton Dickinson and Co., Lincoln Park, NJ). These stock cells were subcultivated before reaching confluence. The medium consisted of Dulbecco's Modified Eagle's Medium (Sigma) supplemented with 10% fetal bovine serum (ICN Biomedicals, Inc, Aurora, OH) and 100 IU/mL penicillin–100 μg/mL streptomycin (Sigma). The monolayer cultures were grown in an atmosphere of 5% CO_2–95% air at 37 °C. The cells were given fresh growth medium every 2 days. When the A549 cells had reached confluence, they were harvested with 0.25 mM trypsin and 0.2% EDTA (0.5–1 min at 37 °C), resuspended, and seeded into a new flask. For the uptake study, A549 cells were seeded at a cell density of 1×10^5 cells/cm^2 on 24-well plates (Corning Costar Corp., Cambridge, MA). The cell monolayers were fed a fresh growth medium every 2 days and were used at 4 to 6 days for the uptake experiments.

2.3. Uptake study in A549 cell monolayers

The uptake of AMD was measured using monolayer cultures grown in 24-well plates. The incubation medium used for the uptake study was HBSS-MES buffer (pH 5.0) (25 mM D-glucose, 137 mM NaCl, 5.37 mM KCl, 0.3 mM Na_2HPO_4, 0.44 mM KH_2PO_4, 1.26 mM $CaCl_2$, 0.8 mM $MgSO_4$ and 10 mM MES). After removal of the growth medium, cells were preincubated at 37 °C for 10 min with 0.5 mL of HBSS-MES buffer (pH 5.0). After removal of the medium, 0.5 mL of incubation medium containing AMD or [^{3}H] E-3-S was added. The monolayers were incubated for the indicated time at 37 °C. Each cell monolayer was washed rapidly twice with an ice-cold incubation medium at the end of the incubation period. To quantify the concentration of AMD, the cells were solubilized with 0.25 mL of 1 N NaOH and neutralized with 0.25 mL of 1 N HCl. After vortexing briefly, a part of the mixture (100 μL) was transferred to a fresh tube and 400 μL MeOH was added. After centrifugation of the mixture (12,000×g for 10 min), the concentrations of AMD in the supernatant were measured. To quantify the radioactivity of [^{3}H] E-3-S, the cells were solubilized in 1% SDS / 0.2 N NaOH. The remainder of the sample was mixed with 8 mL of scintillation cocktail (Amersham International, UK) to measure the radioactivity. All the uptake values were corrected against protein content.

2.4. RT-PCR analysis

RT-PCR was performed as described previously [25]. Total RNA was prepared from A549 cells using an ISOGEN (Nippon Gene, Tokyo) and an RNase-Free DNase Set (QIAGEN). Single-strand cDNA was made from 2 μg total RNA by reverse transcription (RT) using a ReverTraAce (TOYOBO, Japan). Gene-specific primers for OATP1A2, OATP2B1,

OATP1B1, OATP3A1, OATP4A1 and OATP1B3 are shown in Table 1. For OATP3A1 and OATP4A1, the experimental conditions were validated by demonstrating the formation of RT-PCR products of the expected sizes with total RNA of HepG2 cells as a positive control. PCR was performed using Hot Star Taq PCR (QIAGEN) through 35 cycles of 94 °C for 15 s, 58 °C (for OATP1A2, OATP2B1, OATP3A1, and OATP1B3) or 55 °C (for OATP1B1 and OATP4A1) for 30 s, and 72 °C for 30 s. The PCR products were subjected to electrophoresis on a 2% agarose gel and then visualized by ethidium bromide staining.

2.5. Quantitative real-time PCR

Quantitative real-time PCR was performed as described previously [25]. Quantitative real-time PCR was performed using an ABI PRISM 7700 sequence detector (Applied Biosystems) with 2×SYBR Green PCR Master Mix (Applied Biosystems) and specific primers for OATP2B1 (sequence shown in Table 1) and GAPDH (forward: 5′-AAG GTC ATC CCT GAG CTG AA-3′ and reverse: 5′-TTC TAG ACT TCA TTG CAG GT-3′) as per the manufacturer's protocol. A three-step temperature program was applied for the amplification of OATP2B1 and GAPDH: initial denaturation (95 °C) for 10 min and then 94 °C for 15 s, 58 °C for 30 s and 72 °C for 30 s for 40 cycles.

2.6. OATP2B1 small interfering RNA (siRNA) and siRNA transfection

Three kinds of siRNA (117442, 120018 and 120019) targeted to different regions of the OATP2B1 gene and nontargeting siRNA (AM4635) as a negative control were purchased from Ambion. Delivery of siRNAs into A549 cells was performed by reverse transfection methods as per the manufacturer's protocol. One μL siPORT NeoFX (Ambion) and 49 μL Opti-MEM I medium (Invitrogen) were mixed and incubated at room temperature for 10 min. Two μM siRNA was diluted to 300 nM with Opti-MEM I medium. Fifty μL diluted siPORT NeoFX and 50 μL diluted siRNA were mixed and incubated for 10 min, and then these complexes were dispensed into the wells of a 24-well plate and 400 μL of suspended A549 cells (1.5×10^5 cells/mL) was transferred. Following siRNA transfection (24 h), the medium was replaced with fresh normal growth medium and then the cells were used for analysis and experimentation at the times indicated.

2.7. Analytical procedures

AMD was determined using an HPLC system equipped with a Shimadzu LC liquid chromatograph pump and UV detector. The
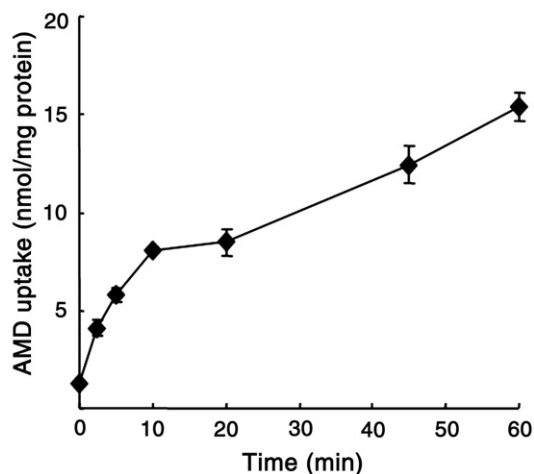

Fig. 1. Time course of AMD uptake by A549 cells. The uptake of AMD (25 μM) was measured at pH 5.0 at 37 °C. Each point represents the mean ± S.D. of 3 independent experiments.
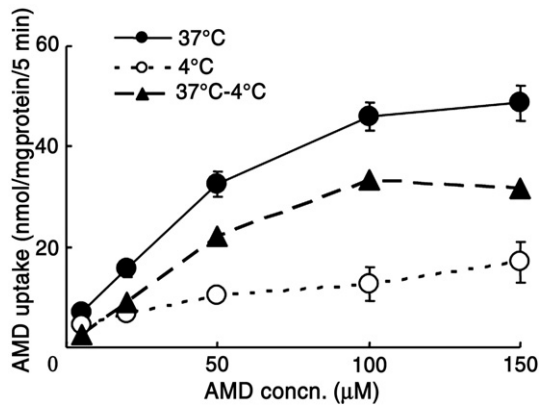
Fig. 2. Concentration-dependence of AMD uptake by A549 cells. The uptake of AMD was measured for 5 min at pH 5.0 at 37 °C (closed circles) or 4 °C (open circles). Triangles represent the difference between the uptake at 37 °C and that at 4 °C. Each point represents the mean ± S.D. of 3 independent experiments.

column was a Mightysil RP-8GP column (4.6 × 250 mm (5 μm), Kanto Chemical). A mobile phase containing 9.5 mM H_3PO_4: acetonitrile (1:1, v/v) was used. Column temperature and flow rate were 40 °C and 1.0 mL/min, respectively. The wavelength for detection of AMD was 242 nm. Radioactivity was determined using a liquid scintillation counter (Packard, 1600TR). Protein was measured by the method of Lowry et al. with bovine serum albumin as a standard [29].

Statistical significance was evaluated using ANOVA followed by Dunnett test, and a value of $P < 0.05$ was considered significant. Nonlinear regression analysis was performed by using Origin® (version 6.1J).

Kinetic parameters were obtained using the following equation:

$$v = V_{max} \times s / (K_m + s) + K_{ns} \times s$$

where v is the uptake rate of compounds, s is the compounds concentration in the medium, K_m is the Michaelis–Menten constant and V_{max} is the maximam uptake rate. K_{ns} represents non-saturable uptake clearance.

3. Results

3.1. Uptake of AMD by A549 cells

In the first part of this study, AMD uptake by A549 cells was measured. Fig. 1 shows the time courses of the uptake of AMD. The uptake of AMD linearly increased for 10 min after the start of
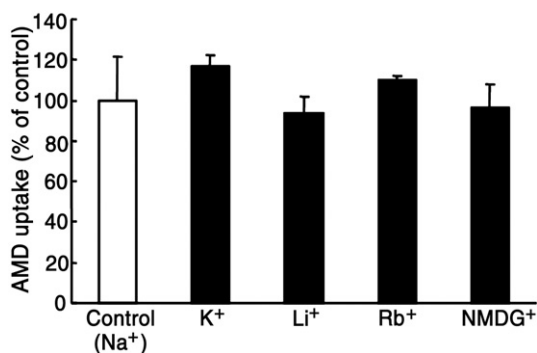

Fig. 3. Effects of extracellular cations on the uptake of AMD by A549 cells. A549 cells were incubated with AMD (25 μM) for 5 min at pH 5.0 at 37 °C. The results were normalized by the uptake in the presence of Na^+. Each column is expressed by the mean with S.D. of 3 independent experiments.

Table 2
Inhibitory effects of various compounds on the uptake of AMD by A549 cells.

Inhibitor	Concentration	AMD uptake
	mM	% of control
TEA	5.0	120.9 ± 3.2[**]
Choline	5.0	128.6 ± 2.6[**]
Cimetidine	5.0	99.9 ± 6.9
PAH	5.0	90.2 ± 6.8
BSP	0.5	25.9 ± 1.5[**]
E-3-S	0.5	47.1 ± 1.8[**]
DHEAS	0.5	47.4 ± 0.3[**]
Benzylpenicillin	10.0	71.9 ± 8.5[*]
Pravastatin	5.0	57.2 ± 11.5[**]
DIDS	0.5	34.6 ± 1.9[**]
Indomethacin	0.5	29.4 ± 5.9[**]
Valproic acid	10.0	47.2 ± 8.1[**]
Taurocholate	2.5	78.9 ± 5.3
T_3	0.1	97.6 ± 3.2
$E_217\beta G$	0.1	98.0 ± 5.6

A549 cells were incubated with AMD (25 μM) for 5 min at 37 °C at pH 5.0. Each value is the mean ± S.D. of 3–9 independent experiments.
 [*] Significantly different from control ($p < 0.05$).
 [**] Significantly different from control ($p < 0.01$).

incubation. Thus, the initial uptake was evaluated for 5 min. To obtain kinetic parameters, the concentration-dependence of the uptake of AMD by A549 cells was examined. The uptake of AMD after subtraction of the value at 4 °C was saturated (Fig. 2) and the apparent K_m and V_{max} values were 66.8 ± 30.3 μM and 49.7 ± 9.7 nmol/mg protein/5 min, respectively. To characterize the transport mechanisms of AMD, the effect of replacement of Na^+ with various cations on the uptake of AMD was examined. When Na^+ was replaced with K^+, Li^+, Rb^+ or N-methyl-D-glucamine, the uptake of AMD was not significantly different from that in the presence of Na^+ (Fig. 3), suggesting an Na^+-independent transport mechanism.

3.2. Effects of various compounds on the uptake of AMD by A549 cells

To determine the mechanism of AMD transport, the inhibitory effects of various compounds were examined (Table 2). Since AMD is a cation, firstly, we investigated whether substrates of organic cation transporters (OCTs) inhibited the uptake of AMD. Tetraethylammonium (TEA) and choline, substrates of OCTs, did not inhibit the uptake of AMD but rather slightly increased it. Cimetidine also had no effect on AMD uptake. On the other hand, the uptake of AMD was significantly inhibited by the OATP substrates, sulfobromophtalein (BSP), estrone-3-sulfate (E-3-S), dehydroepiandrosterone-sulfate (DHEAS), benzyl-penicillin and pravastatin but not by triiodothyronine (T_3) and estradiol-17β-glucuronide ($E_217\beta G$). 4,4′-diisothiocyanostilbene-2,2′-disulfonic acid (DIDS), indomethacin and valproic acid also exhibited inhibitory effects, and taurocholate slightly inhibited the uptake of AMD. However, the organic anion transporter (OAT) substrate p-aminohippurate (PAH) had no effect on the uptake of AMD. The inhibition profiles were similar to the inhibitory effects of those compounds on OATP2B1-mediated E-3-S transport [27].
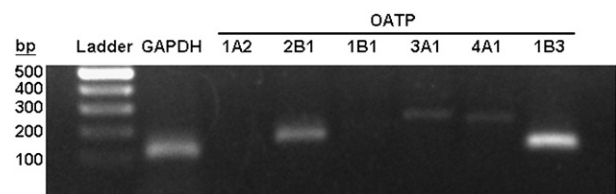

Fig. 4. Expression of OATP transporters in A549 cells. RT-PCR was performed with total RNA isolated from A549 cells. Specific primers were used to detect genes as described in Materials and methods.
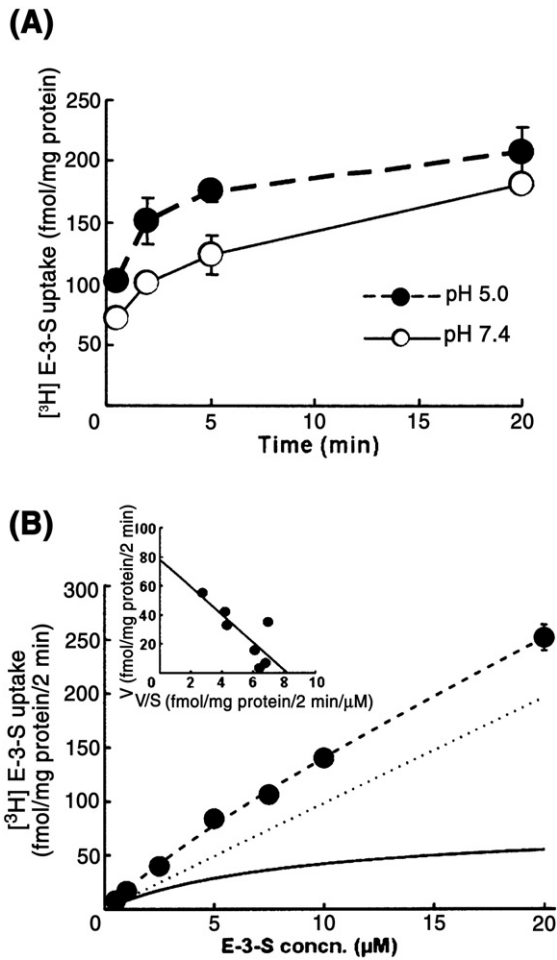
Fig. 5. (A) Time course of [^{3}H]E-3-S uptake by A549 cells. The uptake of [^{3}H]E-3-S (5.0 nM) was measured at pH 7.4 (open circles) or pH 5.0 (closed circles) at 37 °C. Each point represents the mean ± S.D. of 3 independent experiments. (B) Concentration-dependence of [^{3}H]E-3-S uptake by A549 cells. The uptake of [^{3}H]E-3-S was measured for 2 min at pH 5.0 at 37 °C. Dotted and solid lines represent the nonsaturated and saturated uptakes, respectively, obtained from nonlinear least-square regression analysis of the total uptake (closed circles). An Eadie–Hofstee plot of [^{3}H]E-3-S uptake after subtraction of the estimated non-saturable component is shown in the inset. Each point represents the mean ± S.D. of 3 independent experiments.

3.3. Identification of transporters expressed in A549 cells

To investigate subtypes of OATPs involved in AMD transport in A549 cells, the mRNA expressions of several OATPs were investigated by RT-PCR analysis. As shown in Fig. 4, RT-PCR analysis demonstrated mRNA expression of OATP2B1 and 1B3 in A549 cells. The mRNA expressions of 3A1 and 4A1 were weak and those of 1A2 and 1B1 were not detected. Taking the inhibition profiles of the uptake of AMD into consideration, we suggest that OATP2B1 is a candidate to mediate the uptake of AMD in A549 cells among these OATPs.

Table 3
Effects of various compounds on [^{3}H]E-3-S uptake by A549 cells.

Compound	Concentration	[^{3}H]E-3-S uptake
	mM	% of control
E-3-S (unlabeled)	0.5	57.0 ± 3.8[**]
BSP	0.5	56.7 ± 3.4[**]
DHEAS	0.5	67.2 ± 9.6[**]

A549 cells were incubated with [^{3}H]E-3-S (5.0 nM) for 2 min at pH 5.0 at 37 °C. Each value represents the mean ± S.D. of 3 independent experiments.
[**] Significantly different from control ($p < 0.01$).

3.4. Uptake of E-3-S by A549 cells

We then examined the kinetic analysis of the uptake of [^{3}H] E-3-S, which is a model substrate of OATP2B1, in A549 cells. The uptake of [^{3}H]E-3-S by A549 cells at pH 5.0 was higher than that at pH 7.4. (Fig. 5A) This result is consisted with the previous report that OATP2B1 has higher activity at acidic pH than neutral pH [30]. Furthermore, the
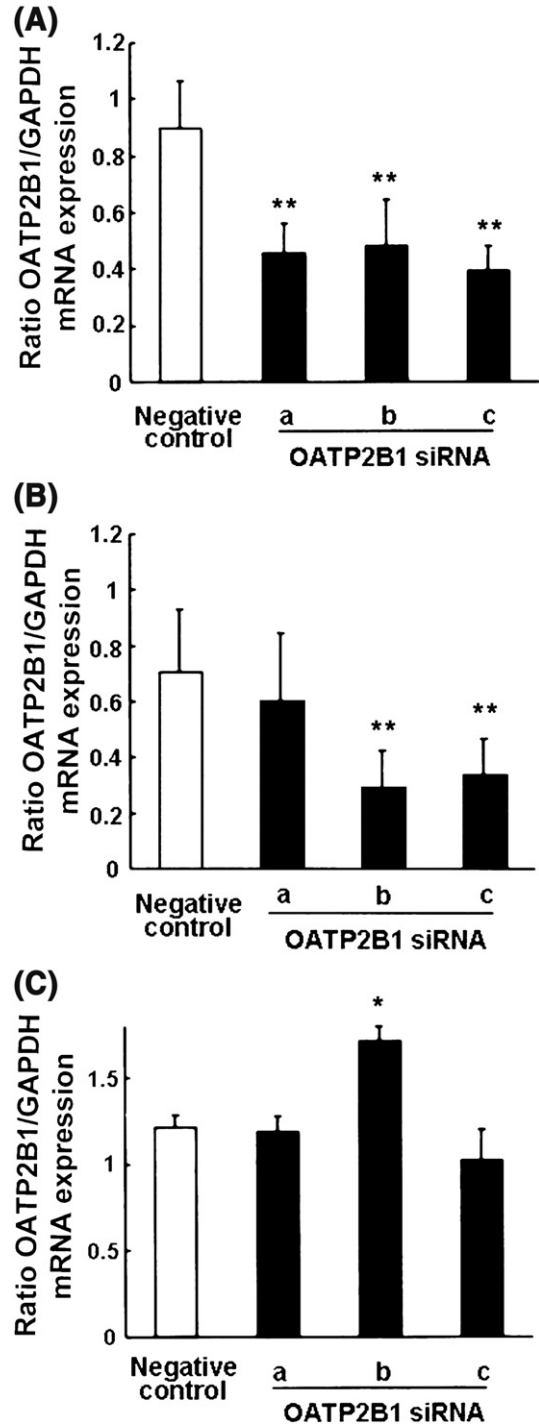

Fig. 6. Analysis of siRNA-mediated silencing of OATP2B1 mRNA expression by quantitative real-time RT-PCR at 48 (A), 72 (B) and 96 h (C) after transfection. Expression analyses were performed using three different siRNA constructs, OATP2B1-a, b and c. OATP2B1 mRNA expression levels were normalized to GAPDH in A549 cells. Each column represents the mean with S.D. of 3–6 independent experiments. *; significantly different from negative control siRNA ($p < 0.05$). **; significantly different from negative control siRNA ($p < 0.01$).
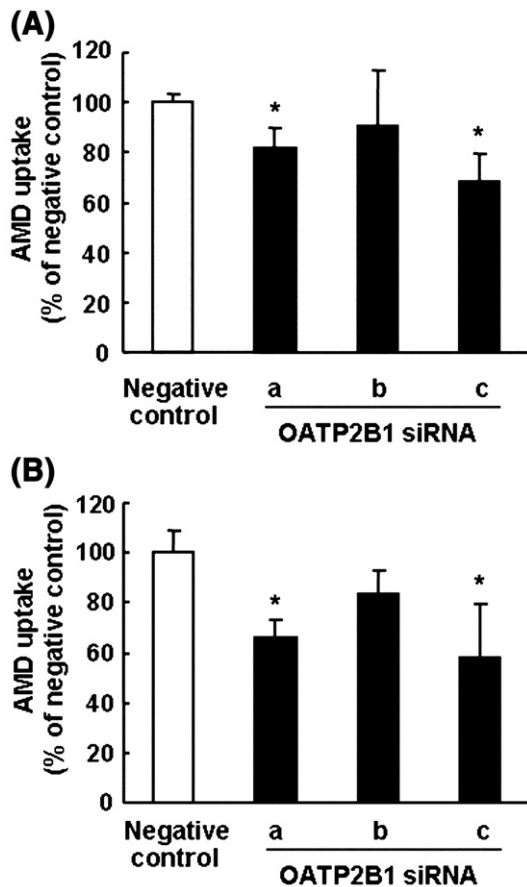
(A)

(B)

Fig. 7. Effect of OATP2B1 siRNA on AMD uptake in A549 cells at 48 (A) and 72 h (B) after transfection. A549 cells were treated with negative control siRNA or OATP2B1 siRNA. The uptake studies were performed at 48 (A) and 72 h (B) after transfection. The uptake of AMD (25 μM) was evaluated for 5 min at pH 5.0 and expressed as the difference between the uptake at 37 °C and that at 4 °C. The results were normalized by the uptake in the negative control siRNA-treated A549 cells. Each column represents the mean with S.D. of 3 independent experiments. *; significantly different from negative control siRNA ($p<0.05$).

uptake of [³H]E-3-S was significantly inhibited by unlabeled E-3-S, BSP and DHEAS, which are substrates for OATP2B1 (Table 3). Initial uptake (2 min) of [³H]E-3-S by A549 cells at concentrations ranging 0.5 to 20 μM exhibited saturation at pH 5.0. Eadie–Hofstee plots showed a single straight line, and the K_m and V_{max} were 8.8 ± 2.5 μM and 79.2 ± 10.4 fmol/mg protein/2 min, respectively (Fig. 5B).

3.5. Effects of OATP2B1 siRNA on OATP2B1 mRNA expression and AMD uptake in A549 cells

To investigate whether OATP2B1 knockdown induces any change in OATP2B1 mRNA expression and AMD uptake in A549 cells, quantitative real-time RT-PCR experiments were performed to quantify OATP2B1 mRNA values at 48, 72 and 96 h after siRNA transfection. In this study, three different siRNA constructs targeted to the *OATP2B1* gene, OATP2B1-a, b and c, were used. The negative control siRNA did not affect OATP2B1 mRNA expression compared with that in cells not transfected with siRNA at 48, 72 and 96 h after transfection (data not shown). Therefore, we used this siRNA as a negative control in this study. Application of three siRNAs for OATP2B1 resulted in a considerable decrease in OATP2B1 mRNA expression level at 48 h after transfection (Fig. 6A). The gene silencing effects of OATP2B1-b and c continued at least until 72 h after transfection (Fig. 6B), whereas those effects appeared to be attenuated at 96 h (Fig. 6C). Thus, we investigated the effects of OATP2B1 siRNA on AMD uptake at

48 and 72 h after transfection. Since the negative control siRNA did not affect AMD uptake compared with that in untreated A549 cells, the results of AMD uptake were normalized to negative control siRNA-treated A549 cells. The uptake of AMD by A549 cells was decreased by transfection of the three different siRNAs at both 48 (up to about 30%) (Fig. 7A) and 72 h (up to about 40%) (Fig. 7B) after transfection. The inhibitory effects at 72 h seemed to be stronger than those of 48 h. To clarify the involvement of OATP2B1 in the inhibitory effects of OATP substrates, as shown in Table 2, the effect of BSP on AMD uptake in OATP2B1-knockdown A549 cells was examined. The AMD uptake was determined at 72 h after transfection, and we used 4 μM BSP, which is a concentration close to IC₅₀ of BSP (5.3 ± 0.2 μM) on AMD uptake by A549 cells. AMD uptake in OATP2B1 siRNA-treated A549 cells was not inhibited by BSP, whereas that in negative control siRNA-treated A549 cells was significantly inhibited (Fig. 8). We confirmed the effect OATP2B1 knockdown on the mRNA expression level of OATP1B3, 3A1 and 4A1 by Real-Time PCR. OATP2B1 siRNA did not reduce these OATPs mRNA expression level (data not shown).

4. Discussion

AMD is a highly effective drug for the treatment of cardiac dysrhythmias, but AMD has several side effects. Pulmonary toxicity is the most life-threatening and limits clinical use of AMD [31–33]. In this study, we focused on the strong tendency of AMD to accumulate in lung tissue and we investigated the AMD uptake mechanism using A549 cells. A549 cell is a model of the type II alveolar epithelial cell (AEC), which possesses many lung functions, including antioxidant defense and lung specific phospholipids comprising pulmonary surfactant. In addition, AECs are stem cells for alveolar epithelial repair after lung injury and during normal AEC turnover [34]. Dysfunction of the AEC repair system or cytotoxicity for AECs may lead to acceleration of collagen deposition and lung fibroblast proliferation [35]. AMD-induced cytotoxicity for AECs might be a critical factor in the pathogenesis of AIPT [34,35]. Therefore, carrier-mediated AMD uptake, which we found in this study, might lead to an increase in the incidence of AIPT. This mechanism might also be
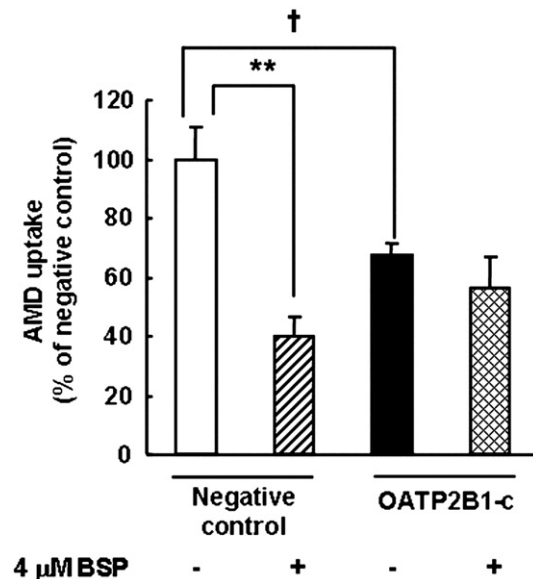

Fig. 8. Effect of BSP on the uptake of AMD by negative control siRNA- and OATP2B1 siRNA-treated A549 cells. The uptake studies were performed at 72 h after transfection. The uptake of AMD (25 μM) was evaluated at 5 min at pH 5.0 and expressed as the difference between the uptake at 37 °C and that at 4 °C. The results were normalized by the uptake in the negative control siRNA-treated A549 cells. Each column represents the mean with S.D. of 3 independent experiments. **; significantly different from the absence of BSP ($p<0.01$). †; significantly different from negative control siRNA ($p<0.05$).

involved in the AMD accumulation in lung alveolar epithelial cells. We characterized this mechanism considering as a new aspect of pharmacokinetic feature of AMD.

Although AMD charges positively under the physiologic condition, the uptake of AMD was inhibited by OATP substrates, BSP, E-3-S and DHEAS [36–38] (Table 2). These anionic compounds are also OAT substrates, but PAH, which is a typical substrate of OATs, did not exhibit an inhibitory effect, indicating that AMD uptake was affected by OATPs but not by OATs. On the other hand, T_3, a typical substrate of most OATPs [36–39], had no effect on the uptake of AMD. Although mRNA expression of several OATPs (OATP2B1, 3A1, 4A1 and 1B3) was observed in A549 cells (Fig. 4), only OATP2B1 among human OATPs does not transport thyroid hormones (OATP2A1, 5A1 and 6A1 have not been fully investigated) [39,40]. $E_2 17\beta G$, which is a substrate or an inhibitor of OATP1B3 but not OATP2B1 [41], did not exhibit an inhibitory effect on AMD uptake, indicating that OATP1B3 has little influence on AMD uptake. OATP2B1 has been reported to be expressed in a variety of tissues, including the lung [28,40], and BSP, E-3-S and DHEAS are well-known substrates for OATP2B1 [40]. The K_m value for [^{3}H]E-3-S uptake by A549 cells is similar to the reported K_m value for [^{3}H]E-3-S uptake by HEK293 cells expressing OATP2B1 at pH 5.0 (13.1 ± 3.2 μM) (Fig. 5) [30]. These results indicate that OATP2B1 is active in A549 cells. In this study, BSP inhibited the uptake of AMD with an IC$_{50}$ value of 5.3 ± 0.2 μM (data not shown). This IC$_{50}$ value is not greatly different from the reported K_m value for BSP uptake by OATP2B1-injected *Xenopus laevis* oocytes (0.7 μM) [40]. Thus, we investigated the effects of other OATP2B1 substrates (benzylpenicillin and pravastatin) and inhibitors (taurocholate, DIDS, indomethacin and valproic acid) [27,42]. All of the tested compounds except taurocholate significantly inhibited AMD uptake (Table 2). The transport mechanism of AMD was Na$^+$-independent (Fig. 3), and this is also consistent with the fact that OATPs are Na$^+$-independent transporters [36–38].

Based on these results, we hypothesized that OATP2B1 is involved in the uptake of AMD in A549 cells. Due to the low solubility of AMD, it was difficult to perform further kinetic analysis. Thus, to investigate whether OATP2B1 mediates AMD uptake, OATP2B1 knockdown in A549 cells was examined by using siRNA.

The siRNAs targeted to the *OATP2B1* gene reduced OATP2B1 mRNA expression level in A549 cells up to about 50% (Fig. 6) and the uptake of AMD up to about 40% (Fig. 7). Since OATP2B1 siRNA did not reduce other OATPs mRNA expression level (data not shown), it is considered that the decrease of AMD uptake in OATP2B1 siRNA-treated A549 cells was the result of OATP2B1 knockdown, and OATP1B3, 3A1 and 4A1 did not affect AMD uptake. In addition, the inhibitory effect of BSP on AMD uptake was attenuated in OATP2B1 siRNA-treated A549 cells, compared to that in negative control siRNA-treated A549 cells (Fig. 8), indicating that the inhibitors of AMD uptake, as shown in Table 2, might inhibit OATP2B1-mediated AMD uptake. Although general Oatp/OATP substrates are mainly anionic amphipathic molecules, there are several Oatps/OATPs that transport organic cations (e.g., N-(4,4-azo-*n*-pentyl)-21-deoxyajmalinium and N-methylquinidine) [37,43]. We speculate that OATP2B1 also transports or interacts with cationic compounds like AMD as well as anionic compounds. These results may provide new insight into OATP2B1 function. Although the apparent K_m value of AMD transport in A549 cells was 66.8 ± 30.3 μM, the K_m value for transport of AMD by OATP2B1 was not obtained in this study. In addition, the involvement of uptake mechanisms other than OATP2B1 cannot be excluded. Further experiments are required to clarify the accurate kinetic parameter values for transport of AMD by OATP2B1 and to compare the K_m value of AMD to the therapeutic serum level of AMD (2.99 μM) with the general dose of 400 mg/day [44].

In clinical practice, it is important to be aware of the potential of drug–drug interactions and variations in the pharmacological effects of drugs by genetic polymorphisms. One single nucleotide polymorphism in the *OATP2B1* gene was reported to influence the transport activity [45]. Alteration of AMD uptake activities in the lung by genetic polymorphisms could cause interindividual difference in AIPT incidence. In addition, recent studies have shown that several drugs are recognized by or interact with OATP2B1 [43,46–48]. It is likely that the transport process of AMD is inhibited by co-administered drugs, resulting in alteration of AMD pharmacokinetics. The information of the AMD uptake mechanism obtained in this study will be useful for resolving the difficulty in control of AMD serum level [9].

In summary, AMD was transported by a carrier-mediated system into A549 cells, and OATP substrates and inhibitors inhibited the AMD uptake. Transport of AMD by A549 cells is mainly mediated by OATP2B1. The newly found pharmacokinetic feature of AMD may be a key to explain the mechanism of AMD accumulation in the lung and the high incidence of AIPT.

References

[1] J.M. Herre, M.J. Sauve, P. Malone, J.C. Griffin, I. Helmy, J.J. Langberg, H. Goldberg, M.M. Scheinman, Long-term results of amiodarone therapy in patients with recurrent sustained ventricular tachycardia or ventricular fibrillation, J. Am. Coll. Cardiol. 13 (1989) 442–449.

[2] S.N. Singh, R.D. Fletcher, S.G. Fisher, B.N. Singh, H.D. Lewis, P.C. Deedwania, B.M. Massie, C. Colling, D. Lazzeri, Amiodarone in patients with congestive heart failure and asymptomatic ventricular arrhythmia. Survival trial of antiarrhythmic therapy in congestive heart failure, N. Eng. J. Med. 333 (1995) 77–82.

[3] L. Ceremuzynski, E. Kleczar, M. Krzeminska-Pakula, J. Kuch, E. Nartowicz, J. Smielak-Koromble, A. Dyduszynski, J. Maciejewicz, T. Zaleska, E. Lazarczyk-Kedzia, J. Motyka, B. Paczkowska, O. Sczaniecka, S. Yusuf, Effect of amiodarone on mortality after myocardial infarction: a double-blind, placebo-controlled, pilot study, J. Am. Coll. Cardiol. 20 (1992) 1056–1062.

[4] H.C. Doval, D.R. Nul, H.O. Grancelli, S.V. Perrone, G.R. Bortman, R. Curiel, Randomized trial of low-dose amiodarone in severe congestive heart failure. Grupo de Estudio de la Sobrevida en la Insuficiencia Cardiaca en Argentina (GESICA), Lancet 344 (1994) 493–498.

[5] M.J. Janse, M. Malik, A.J. Camm, D.G. Julian, G.A. Frangin, P.J. Schwartz, Identification of post acute myocardial infarction patients with potential benefit from prophylactic treatment with amiodarone. A substudy of EMIAT (the European Myocardial Infarct Amiodarone Trial), Eur. Heart J. 19 (1998) 85–95.

[6] M. Pfisterer, W. Kiowski, D. Burckhardt, F. Follath, F. Burkhart, Beneficial effect of amiodarone on cardiac mortality in patients with asymptomatic complex ventricular arrhythmias after acute myocardial infarction and preserved but not impaired left ventricular function, Am. J. Cardiol. 69 (1992) 1399–1402.

[7] S.N. Singh, S.G. Fisher, P.C. Deedwania, P. Rohatgi, B.N. Singh, R.D. Fletcher, Pulmonary effect of amiodarone in patients with heart failure. The Congestive Heart Failure-Survival Trial of Antiarrhythmic Therapy (CHF-STAT) Investigators (Veterans Affairs Cooperative Study No. 320), J. Am. Coll. Cardiol. 30 (1997) 514–517.

[8] L.M. Hondeghem, D.J. Snyders, Class III antiarrhythmic agents have a lot of potential but a long way to go. Reduced effectiveness and dangers of reverse use dependence, Circulation 81 (1990) 686–690.

[9] S.J. Connolly, Evidence-based analysis of amiodarone efficacy and safety, Circulation 100 (1999) 2025–2034.

[10] J.W. Mason, Amiodarone, N. Engl. J. Med. 316 (1987) 455–466.

[11] R. Sunderji, Z. Kanji, K. Gin, Pulmonary effects of low dose amiodarone: a review of the risks and recommendations for surveillance, Can. J. Cardiol. 16 (2000) 1435–1440.

[12] T.L. Blake, M.J. Reasor, Acute pulmonary inflammation in hamsters following intratracheal administration of amiodarone, Inflammation 19 (1995) 55–65.

[13] P. Chatelain, R. Laruel, R. Vic, R. Brotelle, Differential effects of amiodarone and propranolol on lipid dynamics and enzymatic activities in cardiac sarcolemmal membranes, Biochem. Pharmacol. 38 (1989) 1231–1239.

[14] T.E. Massey, R.G. Leeder, E. Rafeiro, J.F. Brien, Mechanisms in the pathogenesis of amiodarone-induced pulmonary toxicity, Can. J. Physiol. Pharmacol. 73 (1995) 1675–1685.

[15] I.S. Choi, B.S. Kim, K.S. Cho, J.C. Park, M.H. Jang, M.C. Shin, S.B. Jung, J.H. Chung, C.J. Kim, Amiodarone induces apoptosis in L-132 human lung epithelial cell line, Toxicol. Lett. 132 (2002) 47–55.

[16] M.W. Bolt, J.W. Card, W.J. Racz, J.F. Brien, T.E. Massey, Disruption of mitochondrial function and cellular ATP levels by amiodarone and N-desethylamiodarone in initiation of amiodarone-induced pulmonary cytotoxicity, J. Pharmacol. Exp. Ther. 298 (2001) 1280–1289.

[17] P.C. Adams, D.W. Holt, G.C. Storey, A.R. Morley, J. Callaghan, R.W. Campbell, Amiodarone and its desethyl metabolite: tissue distribution and morphologic changes during long-term therapy, Circulation 72 (1985) 1064–1075.

[18] J.F. Brien, S. Jimmo, F.J. Brennan, S.E. Ford, P.W. Armstrong, Distribution of amiodarone and its metabolite, desethylamiodarone, in human tissues, Can. J. Physiol. Pharmacol. 65 (1987) 360–364.

[19] T.A. Plomp, W.M. Wiersinga, R.A. Maes, Tissue distribution of amiodarone and desethylamiodaone in rats after multiple intraperitoneal administration of various amiodarone dosages, Arzneimittelforschung 35 (1985) 122–129.

[20] T.A. Plomp, W.M. Wiersinga, R.A. Maes, Tissue distribution of amiodarone and desethylamiodaone in rats after repeated oral administration of various amiodarone dosages, Arzneimittelforschung 35 (1985) 1805–1810.

[21] R.V. Martín-Algarra, R.M. Pascual-Costa, M. Merino, V.G. Casabó, Intestinal absorption kinetics of amiodarone in rat small intestine, Biopharm. Drug Dispos. 18 (1997) 523–532.

[22] M. Kakumoto, K. Takara, T. Sakaeda, Y. Tanigawara, T. Kita, K. Okumura, MDR1-mediated interaction of digoxin with antiarrhythmic or antianginal drugs, Biol. Pharm. Bull. 25 (2002) 1604–1607.

[23] T. Kodawara, S. Masuda, H. Wakasugi, Y. Uwai, T. Futami, H. Saito, T. Abe, K. Inui, Organic anion transporter oatp2-mediated interaction between digoxin and amiodarone in the rat liver, Pharm. Res. 19 (2002) 738–743.

[24] S. Funakoshi, T. Murakami, R. Yumoto, Y. Kiribayashi, M. Takano, Role of organic anion transporting polypeptide 2 in pharmacokinetics of digoxin and beta-methyldigoxin in rats, J. Pharm. Sci. 94 (2005) 1196–1203.

[25] M. Kobayashi, I. Fujita, S. Itagaki, T. Hirano, K. Iseki, Transport mechanism for L-lactic acid in human myocytes using human prototypic embryonal rhabdomyo-sarcoma cell line (RD cells), Biol. Pharm. Bull. 28 (2005) 1197–1201.

[26] M.R. Ballestero, M.J. Monte, O. Briz, F. Jimenez, F. Gonzalez-San Martin, J.J. Marin, Expression of transporters potentially involved in the targeting of cytostatic bile acid derivatives to colon cancer and polyps, Biochem. Pharmacol. 72 (2006) 729–738.

[27] Y. Sai, Y. Kaneko, S. Ito, K. Mitsuoka, Y. Kato, I. Tamai, P. Artursson, A. Tsuji, Predominant contribution of organic anion transporting polypeptide OATP-B (OATP2B1) to apical uptake of estrone-3-sulfate by human intestinal Caco-2 cells, Drug Metab. Dispos. 34 (2006) 1423–1431.

[28] I. Tamai, J. Nezu, H. Uchino, Y. Sai, A. Oku, M. Shimane, A. Tsuji, Molecular identification and characterization of novel members of the human organic anion transporter (OATP) family, Biochem. Biophys. Res. Commun. 273 (2000) 251–260.

[29] O.H. Lowry, N.J. Rosebrough, A.L. Farr, R.J. Randall, Protein measurement with the Folin phenol reagent, J. Biol. Chem. 193 (1951) 265–275.

[30] T. Nozawa, K. Imai, J. Nezu, A. Tsuji, I. Tamai, Functional characterization of pH-sensitive organic anion transporting polypeptide OATP-B in human, J. Pharmacol. Exp. Ther. 308 (2004) 438–445.

[31] F.E. Marchlinski, T.S. Gansler, H.L. Waxman, M.E. Josephson, Amiodarone pulmonary toxicity, Ann. Intern. Med. 97 (1982) 839–845.

[32] W.J. Martin, E.C. Rosenow, Amiodarone pulmonary toxicity. Recognition and pathogenesis (Part 2), Chest 93 (1988) 1242–1248.

[33] W.D. Pitcher, Amiodarone pulmonary toxicity, Am. J. Med. Sci. 303 (1992) 206–212.

[34] B.D. Uhal, Cell cycle kinetics in the alveolar epithelium, Am. J. Physiol. Lung Cell. Mol. Physiol. 272 (1997) 1031–1045.

[35] H. Witschi, Responses of the lung to toxic injury, Environ. Health Perspect. 85 (1990) 5–13.

[36] B. Hagenbuch, P.J. Meier, Organic anion transporting polypeptides of the OATP/SLC21 family: phylogenetic classification as OATP/ SLCO superfamily, new nomenclature and molecular/functional properties, Pflugers Arch. 447 (2004) 653–665.

[37] B. Hagenbuch, P.J. Meier, The superfamily of organic anion transporting polypeptides, Biochim. Biophys. Acta 1609 (2003) 1–18.

[38] J. König, A. Seithel, U. Gradhand, M.F. Fromm, Pharmacogenomics of human OATP transporters, Naunyn. Schmiedebergs, Arch. Pharmacol. 372 (2006) 432–443.

[39] B. Hagenbuch, Cellular entry of thyroid hormones by organic anion transporting polypeptides, Best Pract. Res. Clin. Endocrinol. Metab. 21 (2007) 209–221.

[40] G.A. Kullak-Ublick, M.G. Ismair, B. Stieger, L. Landmann, R. Huber, F. Pizzagalli, K. Fattinger, P.J. Meier, B. Hagenbuch, Organic anion-transporting polypeptide B (OATP-B) and its functional comparison with three other OATPs of human liver, Gastroenterology 120 (2001) 525–533.

[41] I. Tamai, T. Nozawa, M. Koshida, J. Nezu, Y. Sai, A. Tsuji, Functional characterization of human organic anion transporting polypeptide B (OATP-B) in comparison with liver-specific OATP-C, Pharm. Res. 18 (2001) 1262–1269.

[42] T. Nishimura, Y. Kubo, Y. Kato, Y. Sai, T. Ogihara, A. Tsuji, Characterization of the uptake mechanism for a novel loop diuretic, M17055, in Caco-2 cells: involvement of organic anion transporting polypeptide (OATP)-B, Pharm. Res. 24 (2007) 90–98.

[43] X. Bossuyt, M. Müller, B. Hagenbuch, P.J. Meier, Polyspecific drug and steroid clearance by an organic anion transporter of mammalian liver, J. Pharmacol. Exp. Ther. 276 (1996) 891–896.

[44] D.W. Holt, G.T. Tucker, P.R. Jackson, G.C. Storey, Amiodarone pharmacokinetics, Am. Heart J. 106 (1983) 840–847.

[45] T. Nozawa, M. Nakajima, I. Tamai, K. Noda, J. Nezu, Y. Sai, A. Tsuji, T. Yokoi, Genetic polymorphisms of human organic anion transporters OATP-C (SLC21A6) and OATP-B (SLC21A9): allele frequencies in the Japanese population and functional analysis, J. Pharmacol. Exp. Ther. 302 (2002) 804–813.

[46] M. Shimizu, K. Fuse, K. Okudaira, R. Nishigaki, K. Maeda, H. Kusuhara, Y. Sugiyama, Contribution of OATP (organic anion-transporting polypeptide) family transporters to the hepatic uptake of fexofenadine in humans, Drug Metab. Dispos. 33 (2005) 1477–1481.

[47] M. Grube, K. Köck, S. Oswald, K. Draber, K. Meissner, L. Eckel, M. Böhm, S.B. Felix, S. Vogelgesang, G. Jedlitschky, W. Siegmund, R. Warzok, H.K. Kroemer, Organic anion transporting polypeptide 2B1 is a high-affinity transporter for atorvastatin and is expressed in the human heart, Clin. Pharmacol. Ther. 80 (2006) 607–620.

[48] K. Kopplow, K. Letschert, J. König, B. Walter, D. Keppler, Human hepatobiliary transport of organic anions analyzed by quadruple-transfected cells, Mol. Pharmacol. 68 (2005) 1031–1038.